Heterometallic Co^{II}-Co^{III}-M^{II} alkoxido-bridged heptanuclear motifs (M=Cu, Zn). Syntheses, crystal structures and magnetic properties

DOI:
10.1016/j.ica.2017.05.077

Document Version
Accepted author manuscript

Heterometallic Co^{II}-Co^{III}-M^{II} alkoxido-bridged heptanuclear motifs (M = Cu, Zn). Syntheses, crystal structures and magnetic properties

Eliza Martin[a], Violeta Tudor[a,*], Augustin M. Madalan[a], Catalin Maxim[a], Floriana Tuna[b], Francesc Lloret[c], Miguel Julve[c,*], Marius Andruh[a,*]

[a] *Inorganic Chemistry laboratory, Faculty of Chemistry, University of Bucharest, Str. Dumbrava Rosie nr. 23, 020464-Bucharest, Romania, E-mail*: marius.andruh@dnt.ro

[b] *School of Chemistry, University of Manchester, Oxford Road, Manchester M13 9PL, UK*

[c]*Departament de Química Inorgànica/Instituto de Ciencia Molecular, Facultat de Química de la Universitat de València, C/ Catedrático José Beltrán 2, 46980 Paterna, València, Spain; E-mail: miguel.julve@uv.es*

Dedicated to Professor Ionel Haiduc on the occasion of his 80th birthday

ABSTRACT

Two new alkoxido-bridged heterometallic complexes of formula $[Co^{II}Co^{III}_3Cu^{II}_3(dea)_6(CH_3COO)_3](ClO_4)_{0.75}(CH_3COO)_{1.25}$ (**1**) and $[Co^{II}_2Co^{III}_2Zn^{II}_3(tea)_2(piv)_6(CH_3O)_2(OH)_2(CH_3OH)_2]\cdot H_2O$ **2** (H_2dea = diethanolamine, H_3tea = triethanolamine and Hpiv = pivalic acid) have been assembled using aminoalcohol ligands. The cationic core in **1** possesses a three-fold crystallographic axis, and it exhibits a set of three copper(II), one cobalt(II) and three cobalt(III) ions arranged as a hexagon of alternating copper(II) and cobalt(III) ions around the central cobalt(II) ion. Each edge of the hexagon is defined by a double alkoxido bridge, the outer one being bis-monodentate with copper(II)-cobalt(III) pair whereas the inner one adopts a tris-monodentate coordination mode linking the Cu(II)-Co(III) pair with the central cobalt(II) ion. The acetate groups act as bidentate ligands towards the copper(II) ions. The intramolecular cobalt(II)-copper(II) separation is 3.157 Å. A hexagon of two cobalt(II), two cobalt(II) and two zinc(II) ions distributed along three types of edges with a central zinc(II) ion occurs in **2**. A tris-modentate alkoxido bridge is involved in all edges together with another bis-monodentate alkoxido bridge (Co^{III}-Co^{II} and Co^{II}-Zn^{II} pairs) and a carboxylate-pivalate bridge in the *syn-syn* conformation. The five coordination at each

peripheral zinc(II) ion is completed by a monodentate carboxylate-pivalate ligand whereas a methoxo group allows to achieve the six-coordination at each cobalt(III) ion. The intramolecular cobalt(II)-cobalt(II) separation through the inner zinc(II) ion is 6.309 Å. The magnetic properties of **1** and **2** have been investigated in the temperature range 1.9-300 K. The exchange interaction between the six-coordinate cobalt(II) and copper(II) ions through the double alkoxido bridges in **1** and that between the six-coordinate cobalt(II) ions across the diamagnetic zinc(II) ion in **2** are found to be ferromagnetic [J = +5.39(5) (**1**) and +1.05(2) cm^{-1} (**2**)], the accidental orthogonality between the interacting magnetic orbitals accounting for this behaviour in the two cases.

Keywords: mixed-valence clusters; cobalt complexes; copper complexes; zinc complexes; magnetic properties.

1. Introduction

The chemistry of homo- and heterometallic clusters with alkoxido bridges generated by the deprotonation of aminoalcohols is very rich [1]. The main interest in such compounds, when the metal ions are paramagnetic, arises from their magnetic properties. First of all, these complexes, which display various nuclearities and spin topologies, are suitable models for the study of the exchange interactions between paramagnetic centres, which provides valuable information on the factors influencing the nature and magnitude of the magnetic interactions. Then, the chemistry of these systems was stimulated by the search for new single molecule magnets (SMMs) with improved performances. Indeed, many relevant SMMs are constructed by using aminoalcohols as ligands [2]. Most of these complexes are serendipitously obtained, since neither the nuclearity, nor the topology of the metallic centres can be predicted. However, they enrich our knowledge with useful information on the aggregation of identical or different metal ions. When cobalt(II) or manganese(II) salts and aminoalcohols are employed as starting materials, mixed-valence Co^{II}-Co^{III} [3] and Mn^{II}-Mn^{III} [4] assemblies often result (the basicity of the aminoalcohols favors the oxidation of the divalent metal ions). In previous papers, we have reported on mixed-valence cobalt clusters of formula $[Co^{II}_4Co^{III}_3(dea)_6(CH_3COO)_3](ClO_4)_{0.75}(CH_3COO)_{1.25}$ [5] and $[Co_4^{II}Co_2^{III}(dea)_2(Hdea)_4)(piv)_4](ClO_4)_2$ [6] (H_2dea = diethanolamine and Hpiv = pivalic acid) fwhich are obtained by using H_2dea in the self-assembly processes. Within the first compound, characterized by a crystallographic three-fold inversion axis, the central cobalt(II) ion is surrounded by six peripheral cobalt atoms, three of them being divalent and the other three trivalent. The structure of the second compound can be described as four face-sharing monovacant and bivacant distorted heterocubane units.

In our attempts to extend this chemistry towards heterometallic motifs, two new Co^{II}-Co^{III}-Cu^{II} and Co^{II}-Co^{III}-Zn^{II} heptanuclear complexes of formula $[Co^{II}Co^{III}_3Cu^{II}_3(dea)_6(CH_3COO)_3](ClO_4)_{0.75}(CH_3COO)_{1.25}$ (**1**) and $[Co^{II}_2Co^{III}_2Zn^{II}_3(tea)_2(piv)_6(CH_3O)_2(OH)_2(CH_3OH)_2]\cdot H_2O$ (**2**) (H_3tea = triethanolamine) were obtained. Herein, we present their preparation and crystal structures together with their magnetic properties as a function of the temperature.

2. Experimental

2.1. Syntheses

All the chemicals used for the present study were purchased from commercial sources and used without further purification. Elemental analyses (C, H, N) were performed on a Perkin Elmer analyzer and the metal contents were determined by atomic absorption spectroscopy spectrometry by means of a EuroEa Elemental Analyser - SpectrAA-280 FS.

*2.1.1. Synthesis of $[Co^{II}Co_3^{III}Cu_3^{II}(dea)_6(CH_3COO)_3](ClO_4)_{0,75}(AcO)_{1,25}$ (**1**)*

An ethanolic solution (10 mL) of $Co(CH_3COO)_2{\cdot}4H_2O$ (0.5 mmol) and $NaClO_4$ (1 mmol) was reacted with H_2dea (2 mmol) dissolved in 10 mL of ethanol and triethylamine (4 mmol). To the resulting dark red solution, an ethanolic solution (10 mL) of $Cu(ClO_4)_2{\cdot}6H_2O$ (0.5 mmol) and $NaCH_3COO$ (2 mmol). The final mixture was stirred for 2 h and then it was filtered off. The resulting dark blue solution was allowed to evaporate in the open air for two weeks. Dark blue single crystals appeared after a week by slow evaporation of the solution at room temperature. They were collected and dried in a desiccator over calcium chloride. IR data (KBr, cm^{-1}): 34443vs, 3196vs, 2936m, 2875m, 1627m, 1568m, 1432s, 1120vs, 1091vs, 1065vs, 706w, 636s. Elemental analysis. Calcd. (**1**): $C_{32.50}H_{63}Cl_{0.75}\ Co_4\ Cu_3N_6O_{23.50}$: C 28.53; H 4.60; N 6.14; Co 17.24; Cu 13.94. Found: C 28.13; H 4.40; N 6.16; Co 16.85; Cu 13.30%.

*2.1.2. Synthesis of $[Co_2^{II}Co_2^{III}Zn_3^{II}(tea)_2(Piv)_6(CH_3O)_2(CH_3OH)_2(OH)_2]{\cdot}H_2O$ (**2**)*

A methanolic solution (10 mL) of $Co(ClO_4)_2{\cdot}6H_2O$ (0.5 mmol) was reacted with an methanolic solution (10 mL) of triethanolamine (0.5 mmol) and triethylamine (2 mmol). The mixture was stirred for five minutes and then was mixed with a methanolic solution (10 mL) of $Zn(ClO_4)_2{\cdot}6H_2O$ (0.5 mmol), pivalic acid (2 mmol) and trimethylamine (2 mmol). The final mixture was stirred for two hours and then it was filtered off. The resulting dark red solution was allowed to evaporate in the open air for several days. Dark red crystals were collected and dried in a desiccator over calcium chloride. IR data: 3444s, 2958s, 2926m, 2866m, 1819w, 1579vs, 1561vs, 1483s, 1460s, 1410s, 1226m, 1086w, 1046m, 934w, 899w, 640m, 547w. Elemental analysis. Calcd. $C_{46}H_{74}Co_4N_2O_{24}Zn_3$ (**2**): C 36.60; H 6.36; N 1.85; Co 15.63; Zn 13.01. Found: C 36.13; H 6.74; N 1.85; Co 15.21; Zn 13.80%.

Caution! Perchlorate salts are potentially explosive and they should be handled in small quantities and never heated. The syntheses were carried out at the mmol scale and the crystals were grown by slow evaporation at room temperature.

2.2. Physical measurements

IR spectra (KBr pellets) were recorded on a Tensor 37 spectrophotometer in the 4000-400 cm^{-1} region and UV-Vis spectra were recorded with a Jasco V-670 spectrophotometer. Magnetic susceptibility measurements on polycrystalline samples of **1** and **2** were carried out on a Quantum Design SQUID magnetometer in the temperature range 1.9–300 K. The magnetization measurements for both compounds were performed in the field ranges 0–7 (**1**) and 0-5 T (**2**). The diamagnetic corrections for the constituent atoms were estimated as –618 x 10^{-6} (**1**) and –807 x 10^{-6} cm^3 mol^{-1} (**2**) [per $Co^{II}Co^{III}_3Cu^{II}_3$ (**1**) and $Co^{II}_2Co^{III}_2Zn^{II}_3$ (**1**) units] by using the Pascal's constants [7]. The magnetic data were also corrected for temperature-independent paramagnetism [60 x 10^{-6} cm^3 mol^{-1} per mol of copper(II) ions] and the diamagnetic contribution of the sample holder (a plastic bag).

2.3. X-ray crystallographic analysis

Crystals of **1** and **2** were measured on STOE IPDS II single crystal diffractometer, using graphite-monochromated Mo Kα radiation (λ = 0.71073 Å). The structures were solved by direct methods and refined by full-matrix least-squares techniques based on F^2. The non-H atoms were refined with anisotropic displacement parameters. A summary of the crystallographic data and refinement parameters for **1** and **2** is given in Table 1 whereas selected bond lengths and angles re listed in Tables 2 (**1**) and 3 and S1 (**2**).

3. Results and Discussion

The two compounds, $[Co^{II}Co^{III}_3Cu^{II}_3(dea)_6(CH_3COO)_3](ClO_4)_{0.75}\cdot(CH_3COO)_{1.25}$ (**1**) and $[Co^{II}_2Co^{III}_2Zn^{II}_3(tea)_2(piv)_6(CH_3O)_2(OH)_2(CH_3OH)_2]\cdot H_2O$ (**2**), have been obtained by one-pot reactions involving cobalt(II) and copper(II) [or zinc(II)] salts, the aminoalcohol, and the corresponding carboxylate (acetate or pivalate).

*3.1. Description of the structure of $[Co^{II}Co^{III}_3Cu^{II}_3(dea)_6(CH_3COO)_3](ClO_4)_{0.75}\cdot(CH_3COO)_{1.25}$ (**1**)*

The stoichiometry and general structure of this compound is similar to that of $[Co^{II}_4Co^{III}_3(dea)_6(CH_3COO)_3](ClO_4)_{0.75}(CH_3COO)_{1.25}$, (hereafter abbreviated as $[Co^{II}_4Co^{III}_3]$), previously described by us [5]. Indeed, the structure of **1** (see Figure 1) can be seen as the result of replacing the three peripheral cobalt(II) ions from the related heptanuclear $[Co^{II}_4Co^{III}_3]$ motif by copper(II) ions. The cationic assembly has a three-fold crystallographic axis, and it consists of three copper(II), one cobalt(II) and three cobalt(III) ions arranged as a hexagon of alternating copper(II) (Cu1) and cobalt(III) (Co1) ions around the central cobalt(II) ion (Co2). The tripositive cobalt centres are coordinated by two tridentate dea^{2-} ligands, the donor atoms of each one occupying *facial* positions of the octahedron. The two nitrogen atoms occupy *cis* positions. The cobalt(III) ions are easily identified because the values of the Co–N and Co–O bond lengths are significantly shorter than those involving the divalent cobalt ion. So, whereas the values of the Co1-O and Co1-N bond distances cover the ranges 1.872(3)-1.935(3) and 1.954(4)-1.960(4) Å respectively, the Co2 – O distances vary between 2.068(3) and 2.122(3) Å, confirming the divalent oxidation state of Co2. The di- and trivalent cobalt ions are six-coordinate in a somewhat distorted octahedral geometry. For each dea^{2-} ligand, one alkoxido group which is associated with O2 or O3 connects one cobalt(III) and two copper(II) ions, while the other ones, associated with O1 or O4, act as μ_3 bridges connecting the same outer copper(II) and cobalt(III) ions, and fill up the coordination sphere of the central octahedral cobalt(II) ion. Each copper(II) ion shows a strongly distorted octahedral geometry being coordinated by four alkoxido bridging groups, with Cu1-O distances in the range 1.925(2) - 2.369(3)Å, as well as by a unsymmetrical chelating acetato ligand [the two Cu–O(acetato) distances are 1.971(3) and 2.568(1) Å]. It is interesting to compare these values with the Co^{II}-O(acetato) distances in $[Co^{II}_4Co^{III}_3]$: 2.093(6) and 2.251(6) Å. One of the acetate oxygen atoms (O6) in **1** is semicoordinated to the copper(II) ion. The intramolecular distances between the metal ions are 3.027, 3.157, 3.012 and 5.466 Å for Cu1···Co1, Cu1···Co2, Co1···Co2 and Cu1···Cu1', respectively [symmetry code: (') = 1.5-*z*, 1-*x*, 0.5+*y*].

The analysis of the crystal packing of **1** reveals that the cationic heptanuclear units are connected through hydrogen bonds established between the NH groups from one polynuclear unit and the oxygen atom arising from the chelating carboxylato groups from neighboring units [O6···N2'' = 2.837 Å; ('') = 0.75+*y*, 1.25-*x*, 0.75-*z*] (Figure 2), leading to a supramolecular three-dimensional network where the Cu1···Cu1'' distance is 7.915 Å.

3.2. Description of the structure of $[Co^{II}_2Co^{III}_2Zn^{II}_3(tea)_2(piv)_6(CH_3O)_2(OH)_2(CH_3OH)_2]\cdot H_2O$ (**2**)

Two crystallographically independent heptanuclear assemblies occur in **2**. Because of their geometrical parameters do not differ significantly, we will proceed herein to describe the structure of only one of them. The structure of each heptanuclear motif contains two cobalt(II), two cobalt(III) and three zinc(II) ions as shown in Figure 3 (Figure S1 for the second unit). Two cobalt(II) (Co4 and Co4'), two cobalt(III) (Co3 and Co3') and two zinc(II) (Zn2 and Zn2') ions [symmetry code: (') = 1-*x*, 2-*y*, -*z*] describe a hexagon around the central zinc(II) ion (Zn1). The two tea^{3-} ligands are coordinated to the cobalt(III) ions. The trivalent oxidation state of these two cobalt centres is confirmed by the short Co – O [1.874(4) – 1.920(4) Å] and Co – N [1.904(5) Å] bonds. The three alkoxido groups from the tea^{3-} ligand act as bridges as follows: two alkoxido-oxygen atoms (O14 and O16) connect the Co3 atom with Co4 (O16) and Zn2 (O16) acting as bis-monodentate bridges while the third one (O15) links Co3 with the central Zn1 and peripheral Zn2 atoms adopting a tris-monodentate coordination mode. Each methoxo-oxygen atom from the two CH_3O^- groups connects simultaneously three metal centres [Co3, Zn1 and Co4 through O1M and Co3', Zn1 and Co4' across O1M']. Two of the six pivalate groups act as monodentate ligands against each peripheral zinc(II) ion and the remaining four pivalate acts as single bridges in the *syn-syn* coordination mode connecting the Co3/Co4, Co3'/Co4', Zn2/Co3' and Zn2'/Co4 pairs. The cobalt(III) ion (Co3 and its symmetry related Co3') exhibits the characteristic octahedral geometry, being coordinated by the tea^{3-} ligand, and two oxygen atoms arising from the bridging methoxo and carboxylate groups. Each cobalt(II) ion is also six-coordinate by six oxygen atoms, in a distorted octahedral geometry: O11 (from the hydroxo bridge), O1M (from the methoxo bridge), O14 (from one ethoxo-tea^{3-} arm), O12 and O13 (from two adjacent bridging carboxylate-pivalate), and O33 (monodentate methanol molecule). The peripheral zinc(II) ions are five-coordinate in a distorted trigonal bipyramidal surrounding: two oxygen atoms from the terminal and bridging pivalate ligands, two from the ethoxo bridges, and one from the μ_3-OH ligand. One of the bonds at the zinc(II) ion [Zn2 – O15 = 2.453(4) Å] is significantly longer that the others [values in the range 1.954(4) – 1.998(5) Å]. The central zinc(II) ion is six-coordinate with a distorted octahedral geometry which is built by two μ_3-OH, two μ_3-OCH_3, and two μ_3-ethoxo (tea) bridges. The values of the intramolecular Co3···Co4, Co3···Zn1 and Co4···Zn1 distances are 2.950, 2.994 and 3.155 Å, respectively.

3.3. Spectroscopic and magnetic properties

The solid state electronic spectra of compounds **1**, **2** and [$Co^{II}_4Co^{III}_3$] are shown in Figure 4. The three compounds present an absorption band at ca. 1200 nm, that is assigned to the [$Co^{II}O_6$] chromophore: $^4T_{1g} \rightarrow {}^4T_{2g}$ [8]. The bands observed between 300-800 nm arise form charge transfer and d-d transitions associated to the cobalt(III) and cobalt(II) chromophores. The absorption band of the [$Cu^{II}O_5O'$] chrompohore in **1** is clearly observed at 900 nm.

The $\chi_M T$ vs. T curves for compounds **1** and **2** are displayed in Figures 5 and 6 [χ_M is the magnetic susceptibility per $Co^{II}Co_3{}^{III}Cu_3{}^{II}$ (**1**) and $Co^{II}{}_2Co^{III}{}_2Zn^{II}{}_3$ (**2**) units]. Let us discuss first the magnetic properties of **1**. $\chi_M T$ at room temperature for **1** is equal to 4.23 cm^3 mol^{-1} K. This value is greater than the calculated one for the sum of the spin-only contribution of the high-spin cobalt(II) and the three copper(II) ions, the cobalt(III) ions being diamagnetic [$\chi_M T = 1/8[g^2_{Co}S_{Co}(S_{Co} + 1) + 3g^2_{Cu}S_{Cu}(S_{Cu} + 1)] = 3.12$ cm^3 mol^{-1} K with $S_{Co} = 3/2$, $S_{Cu} = 1/2$ and $g_{Cu} = 2.1$ and $g_{Co} = 2.0$] revealing that a significant orbital contribution to the magnetic moment occurs in **1**. Upon cooling, $\chi_M T$ decreases reaching a minimum of 3.75 cm^3 mol^{-1} K at 28.0 K which is followed by an increase to attain 4.05 cm^3 mol^{-1} K at 6.0 K. Below this temperature, $\chi_M T$ decreases abruptly to reach 3.54 cm^3 mol^{-1} K at 1.9 K. The decrease of $\chi_M T$ in the high temperature range is due to the depopulation of the higher energy Kramers doublets of the six-coordinate cobalt(II) ion whereas its increase after the minimum is unambiguously attributed to a ferromagnetic interaction between the central high-spin cobalt(II) ion and the peripheral copper(II) centres. The fact the value of $\chi_M T$ at the minimum is above the calculated one for a set of four magnetically isolated spin doublets ($\chi_M T$ *ca.* 2.82 cm^3 mol^{-1} K), the six-coordinate cobalt(II) ion below 30 K behaving as an Ising doublet with $S_{eff} = ½$ and $g \approx 4.2$ [9], supports this ferromagnetic interaction. The final decrease of $\chi_M T$ at very low temperatures is due to intermolecular antiferromagnetic interactions and/or zero-field splitting effects of the ground state resulting from the parallel alignment of the interacting local spins.

In order to evaluate the magnetic coupling in **1**, we have used the Hamiltonian of Eq (1)

$$\boldsymbol{H} = \boldsymbol{H}_{\text{spin-orbit}} + \boldsymbol{H}_{\text{axial}} + \boldsymbol{H}_{\text{exchange}} + \boldsymbol{H}_{\text{Zeeman}} \qquad (1)$$

where

$$\boldsymbol{H}_{\text{spin-orbit}} = -\alpha\lambda \boldsymbol{L}_{Co2} \cdot \boldsymbol{S}_{Co2}$$

$$\boldsymbol{H}_{\text{axial}} = \Delta(\boldsymbol{L}^2_{zCo2} - 2/3)$$

$$\boldsymbol{H}_{\text{exchange}} = -J(\boldsymbol{S}_{Co2} \cdot \boldsymbol{S}_{Cu1} + \boldsymbol{S}_{Co2} \cdot \boldsymbol{S}_{Cu2} + \boldsymbol{S}_{Co2} \cdot \boldsymbol{S}_{Cu3})$$

$$\boldsymbol{H}_{\text{Zeeman}} = \beta H[-\alpha \boldsymbol{L}_{Co2} + 2.00\, \boldsymbol{S}_{Co2} + g_{Cu1}\boldsymbol{S}_{Cu1} + g_{Cu2}\boldsymbol{S}_{Cu2} + g_{Cu3}\boldsymbol{S}_{Cu3}]$$

The first term in Eq (1) describes the spin-orbit coupling, λ being the spin-orbit coupling parameter and α an orbital reduction factor defined as $\alpha = A\kappa$. The κ parameter takes into account the reduction of the orbital momentum caused by the delocalization of the unpaired electrons and the A parameter contains the admixture of the upper $^4T_{1g}(^4P)$ state into the $^4T_{1g}(^4F)$ ground state (A = 1.5 and 1 in the weak and strong crystal-field limits, respectively). The inclusion of the A factor is due to the T-P isomorphism [10]. The second term is the one-center operator responsible for the axial distortion of the six-coordinate high-spin cobalt(II) ion in **1** which exhibits a C_3 trigonal symmetry. Under this axial distortion, the triplet orbital $^4T_{1g}$ ground state splits into a singlet $^4A_2$ and a doublet ^4E levels with an energy gap of Δ. Finally, the third term accounts for the exchange coupling between the inner cobalt(II) ion and the peripheral copper(II) centres whereas the last one corresponds to the Zeeman effects.

No analytical expression for the magnetic susceptibility depending on the α, λ, Δ, J and g_{Cu} parameters can be derived and matrix diagonalisation techniques have to be used to determine their values [9c]. The set of best-fit parameters are: α = 1.31(1), Δ = 580(6) cm^{-1}, λ = -151(1)cm^{-1}, gCu = 2.09, J = +5.39(5) cm^{-1} and θ = -1.04(1). It deserves to be noted that $g_{Cu1} = g_{Cu2} = g_{Cu3} = g_{Cu}$ by symmetry reasons and θ is a Curie-Weiss term which was introduced to account for the intermolecular interactions. The magnitude of θ has to be considered as the upper limit for them given that the zero-field splitting of the ground term would also contribute to the observed decrease of $\chi_M T$ in the very low temperature range. Assuming a value of A = 1.40, the deduced value of κ is 0.94. As seen in Figure 5, the calculated curve with these parameters matches well the experimental data in the whole temperature range investigated.

The shape of the magnetization (M) against H plot at 2.0 for **1** (see inset of Fig. 5) agrees with the presence of weak intermolecular antiferromagnetic interactions and or zero-field splitting effects, the value of M at 7 T (ca. 4.9 μ_B), being close to the expected saturation value

for the full population of the ground state resulting from the parallel alignment of the cobalt(II) and the three copper(II) local spins.

The values of the α, Δ and λ parameters are within the range of those reported for other high-spin octahedral cobalt(II) complexes [5,9b,c,10,11]. As far as the weak intramolecular ferromagnetic coupling observed, simple orbital symmetry considerations allow us to figure out its origin. Let us to focus first on the Cu1-Co2 pair. The unpaired electron of the Cu1 centre is described by a $d(x^2-y^2)$ type magnetic orbital which is delocalized in the equatorial plane, the *x* and *y* axes being roughly defined by the O5-Cu1-O1 and O2-Cu1-O3 vectors. Given that the spin density at the O4 and O6 axial positions is negligible, the exchange pathway between Cu1 and Co2 would involve the alkoxo O1 atom. Dealing with the high-spin cobalt(II) ion, it has three unpaired electrons ($t_{2g}^4e_g^2$ electronic configuration in O_h symmetry). Due to symmetry reasons, the interaction of the two e_g magnetic orbitals of the cobalt(II) ion with the magnetic orbital of each copper(II) ion will determine the nature of the magnetic interaction observed. As the Cu1-O2-Co2 angle is 96.54(13)º, assuming that the *x* and *y* axes at the cobalt(II) ion are roughly defined by the Co2-O1 and Co2-O4 bonds, an accidental orthogonality between the $d(x^2-y^2)$ magnetic orbitals from Co2 and Cu1 through the O1 bridge would occur, and then a ferromagnetic coupling is expected. The same conclusion is obtained if one considers that the dz^2 magnetic orbital of the cobalt(II) ion is defined by the O1-Co2-O4" vector. These considerations apply to the interactions of the symmetry-related Cu1' and and Cu" atoms with Co2 through the O1' and O1" bridges.

$\chi_M T$ at room temperature for **2** is 6.15 cm^3 mol^{-1} K, a value that is again higher than the spin-only value [ca. 3.75 cm^3 mol^{-1} K for two high-spin cobalt(II) ions with $S_{Co} = 3/2$ and $g_{Co} = 2.0$], in agreement with the expected orbital contribution of the $^4T_1$ ground state for six-coordinate cobalt(II) ions, the cobalt(III) and zinc(II) ions being diamagnetic. Upon cooling, $\chi_M T$ remains practically constant down to 190 K, then decreases to reach 5.0 cm^3 mol^{-1} K at 20 K. Below 20 K, $\chi_M T$ increases to 5.39 cm^3 mol^{-1} K at 3.0 K and it further decreases to 4.97 cm^3 mol^{-1} K at 1.9 K. This behaviour indicates a ferromagnetic coupling between the two cobalt(II) ions across the diamagnetic zinc(II) ion, a conclusion which is based on the fact the the value of $\chi_M T$ at the minimum is well above the calculated value for two magnetically isolated Ising doublets, each one with $S_{eff} = 1/2$ and $g \approx 4.2$ ($\chi_M T$ ca. 3.31 cm^3 mol^{-1} K). The decrease of $\chi_M T$ in the high temperatures domain is due to the depopulation of the higher energy Kramer's doublets of the

cobalt(II) centres whereas that at very low temperatures is attributed to weak intermolecuar antiferromagnetic interactions and/or zero field splitting effects of the ground spin state resulting from the paralell alignment of the two Ising doublets.

Having in mind these considerations, we analyzed the magnetic data of **2** through the Hamiltonian of Eq (2)

$$\boldsymbol{H} = \boldsymbol{H}_{\text{spin-orbit}} + \boldsymbol{H}_{\text{axial}} + \boldsymbol{H}_{\text{exchange}} + \boldsymbol{H}_{\text{Zeeman}} \quad (2)$$

where

$$\boldsymbol{H}_{\text{spin-orbit}} = -\alpha\lambda(\boldsymbol{L}_{\text{Co1}} \cdot \boldsymbol{S}_{\text{Co1}} + \boldsymbol{L}_{\text{Co2}} \cdot \boldsymbol{S}_{\text{Co2}})$$

$$\boldsymbol{H}_{\text{axial}} = \Delta(\boldsymbol{L}^2_{\text{zCo1}} + \boldsymbol{L}^2_{\text{zCo2}} - 4/3)$$

$$\boldsymbol{H}_{\text{exchange}} = -J(\boldsymbol{S}_{\text{Co1}} \cdot \boldsymbol{S}_{\text{Co2}})$$

$$\boldsymbol{H}_{\text{Zeeman}} = \beta H[-\alpha(\boldsymbol{L}_{\text{Co1}} + \boldsymbol{L}_{\text{Co2}}) + 2.00(\boldsymbol{S}_{\text{Co1}} + \boldsymbol{S}_{\text{Co2}})]$$

Again, no analytical expression for the magnetic susceptibility as a function of J, α, λ and Δ can be derived. However, the smaller complexity of the present case compared to the previous one, allowed us to In order to determine the values of these parameters, we used matrix diagonalisation techniques through the *VPMAG* program [12]. The best-fit parameters are: J = +1.05(2) cm^{-1}, α = 1.30(1), Δ = -730(10) cm^{-1} and λ = -134 cm^{-1}. A value of κ = 0.93 is deduced from α = 1.30 and assuming that A = 1.40. The calculated curve reproduces very well the experimental data from room temperature to 3.0 K, in particular both the position and height of the minimum of $\chi_M T$, supporting the validity of the approach used.

The magnetization M versus H plot at 2.0 K [per two cobalt(II) ions] of a polycrystalline sample of **2** is shown in the inset of Figure 6. At 5 T, Compound **2** shows a quasi saturation value of the magnetization at 5 T, M_S = 4.40 μ_B, that is 2.20 μ_B per cobalt(II) ion. This value is smaller than the expected one for a spin quartet with g = 2.0. This is due to the fact that only the Kramer's doublet is populated at 2.0 K. An effective spin S_{eff} =1/2 with a g_{Co} value of 4.2 calculated through the expression $g_{\text{Co}} = (10+2\alpha)/3$ are characteristic for this state leading to $M_S = g_{\text{Co}} S_{\text{eff,Co}} =$ 2.10 μ_B in agreement with the experimental data.

The values of the α, Δ and λ parameters are close to those obtained for **1**. As far as the ferromagnetic coupling between the two high-spin cobalt(II) ions (Co4 and Co4') is concerned [J

= +1.05(2) cm^{-1}]. Orbital symmetry considerations in the light of the structure allow to understand both its nature and magnitude. The exchange pathway responsible for the magnetic coupling between Co4 and Co4' is provided by the O1MO11Zn1O11'O1M' set of atoms. From the three unpaired electrons on each high-spin cobalt(II) ion, the two of e_g symmetry [$d(x^2-y^2)$ and dz^2] are relevant for the magnetic coupling. Focusing on Co4, the *z* axis would be roughly defined by the O13-Co4-O11 vector whereas the Co4-O1M and Co4-O14 bonds would correspond to the the *x* and *y* axes, respectively. The same applies to the symmetry-related Co4' atom. Then, the dz^2 magnetic orbital at Co4 points in a quasi perpendicular manner towards the $d(x^2-y^2)$ magnetic orbital at Co4' through the O11-Zn1-O1M' pathway and the same situation occurs for the dz^2 magnetic orbital from Co4' respect to the $d(x^2-y^2)$ at Co4 across the O11'-Zn1-O1M set of atoms. The accidental orthogonality between these magnetic orbitals of the Co4 and Co4' atoms separated by ca. 6.30 Å would be responsible for the weak ferromagnetic coupling observed in **2**.

4. Conclusions

In conclusion, we synthesised and characterized two new alkoxido-bridged hetrometallic complexes, with interesting topologies. Compound **1** can be seen as resulting from the substitution of three Co(II) ions in the similar [$Co^{II}_4Co^{III}_3$] complex by Cu(II) ions.The investigation of the magnetic properties revealed, for the two compounds, ferromagnetic interactions between the spin carriers, mediated by the alkoxido bridges: Co(II)-Cu(II) (compound **1**) and Co(II)-Co(II) across the diamagnetic Zn(II) ion (compound **2**). In both cases, the ferromagnetic coupling arises from the accidental orthogonality of the magnetic orbitals.

5. Supplementary material

CCDC 1550041 and 1550042 contain the supplementary crystallographic data for **1** and **2**. These data can be obtained free of charge from The Cambridge Crystallographic Data Centre via www.ccdc.cam.ac.uk/data_request/cif.

Acknowledgement

Financial support from the University of Bucharest (Project 741), the Spanish MICINN (Projects CTQ2013-44844P, CTQ2016-75068P and Unidad de Excelencia María de Maetzu

MDM2015-0538) and the Generalitat Valenciana (Project PROMETEOII/2014/070) is gratefully acknowledged.

References

[1] See, for example: (a) G. E. Kostakis, S. P. Perlepes, V. A. Blatov, D. M. Proserpio, A. K. Powell, Coord. Chem. Rev. 256 (2012) 1246;

(b) D. S. Nesterov, O. V. Nesterova, V. N. Kokozay, A. J. L. Pombeiro, Eur. J. Inorg. Chem. 2014, 4496;

(c) G. E. Kostakis, A. K. Powell, Chem. Eur. J. 16, (2010) 7983;

(d) A. Ferguson, J. McGregor, A. Parkin, M. Murrie, Dalton Trans. 2008, 731;

(e) R. Bagai, K. A. Abboud, G. Christou, Chem. Commun. 2007, 3359;

(f) C. M. Kizas, C. Papatriantafyllopoulou, M. Pissas, Y. Sanakis, A. Javed, A. J. Tasiopoulos, C. Lampropoulos, Polyhedron 64 (2013) 280;

(g) W.-G. Wang, A. J. Zhou, W.-X. Zhang, M. L. Tong, X.-M. Chen, M. Nakano, C. C. Beedle, D. N. Hendrickson, J. Am. Chem. Soc. 129 (2007) 1014;

(h) V. A. Milway, F. Tuna, A. R. Farrell, L. E. Sharp, S. Parsons, M. Murrie, Angew. Chem., Int. Ed. 52 (2013) 1949;

(i) D. S. Nesterov, O. V. Nesterova, A. N. Kokozay, A. J. L. Pombeiro, Eur. J. Inorg. Chem. 2014, 4496.

(j) A. Ferguson, J. McGregor, E. K. Brechin, L. H. Thomas, M. Murrie, Dalton Trans. 2009, 9395.

(k) T. Nakajima, K. Seto, F. Horikawa, I. Shimizu, A. Scheuer, B. Kure, T. Kajiwara, T. Tanase, M. Mikuriya, Inorg. Chem. 2012 (51) 12503.

(l) S. Mameri, V. Mereacre, Inorg. Chim. Acta 451 (2016) 52.

(m) D. S. Nesterov, E. C. B. A. Alegria, J. Jezierska, Inorg. Chim. Acta 460 (2017) 83;

(m) C. Jocher, T. Pape, F. E. Hahn, Z. Naturforsch. 60b (2005) 667;

(n) D.-B. Huo, J.– D. Leng, J. Wang, Z.-Z. Wang, W.-M. Lu, X.-S. Hong, A.-J. Zhou, Y.-Y. Lin, J. Coord. Chem. 2017 (70) 936.

[2] (a) E. K. Brechin, Chem. Commun. 2005, 5141;

(b) M. Murrie, Chem. Soc. Rev. 39 (2010) 1986;

(c) L. R. Piquer, E. C. Sañudo, Dalton Trans. 44 (2015) 8771;

(d) S. Goswami, A. K. Mandal, S. Konar, Inorg. Chem. Front. 2 (2015) 687.

[3] Mixed valence Co^{II}-Co^{III} clusters, see for example: (a) A. V. Funes, L. Carrella, L. Sorace, E. Rentschler, P. Alborés, Dalton Trans. 44 (2015) 2390;

(b) S. E. Hosseinian, V. Tangoulis, M. Menelaou, C. P. Raptopoulou, V. Psycharis, C. Dendrinou-Samara, Dalton Trans. 42 (2013) 5355;

(c) S. A. Siddiqi, A. Siddiqi, M. Shahid, M. Khalid, P. K. Sharma, Anjuli, M. Ahmad, S. Kumar, Y. Lan, A. K. Powell, Dalton Trans. 42 (2013) 9513;

(d) L. L. Zheng, J.-D. Leng, R. Herchel, Y.-H. Lan, A. K. Powell, M.-L. Tong, Eur. J. Inorg. Chem. 2010, 2229;

(e) T. R. Barman, M. Sudradhar, M. G. B. Drew, E. Rentschler, Polyhedron 51 (2013) 192.

(f) J.-H. Xu, L.-Y. Guo, H.-F. Su, X. Gao, X.-F. Wu, W.-G. Wang, C. H. Tung, D. Sun, Inorg. Chem. 56 (2017) 1591;

(g) K. G. Alley, R. Bircher, O. Waldmann, S. T. Ochsenbein, H. U. Gu1del, B. Moubaraki, K. S. Murray, F. Fernandez-Alonso, B. F. Abrahams, C. Boskovic, Inorg. Chem., 45 (2006), 8950;

[4] Mixed valence Mn^{II}-Mn^{III} clusters, see for example: (a) T. G. Tziotzi, A. Philippidis, C. P. Raptopoulou, V. Psycharis, C. J. Milios, Polyhedron 64 (2013) 52;

(b) D. I. Alexandropoulos, E. C. Mazarakioti, S. J. Teat, T. C. Stamatatos, Polyhedron 64 (2013) 91.

[5] V. Tudor, G. Marin, F. Lloret, V. Ch. Kravtsov, Yu. A. Simonov, M. Julve, |M. Andruh, Inorg. Chim.Acta 361 (2008) 3446.

[6] V. Tudor, A. Madalan, V. Lupu, F. Lloret, M. Julve, M. Andruh, Inorg. Chim. Acta 363 (2010) 823.

[7] A. Earnshaw, Magnetochemistry, Academic Press, London and New York, 1968.

[8] A. B. P. Lever, Inorganic Electronic Spectroscopy, 2nd Edition, Elsevier, Amsterdam, 1984.

[9] (a) M. E. Lines, J. Chem. Phys. 55 (1971) 2977; (b) R. L. Carlin, Magnetochemistry, Springer-Verlag, Berlin, Hedelberg, 1986; (c) F. Lloret, M. Julve, J. Cano, R. Ruiz-García, E. Pardo, Inorg. Chim. Acta 361 (2008) 3432.

[10] J. M. Herrera, A. Bleuzen, Y. Dromzée, M. Julve, F. Lloret, M. Verdaguer, Inorg. Chem. 42 (2003) 7052.

[11] (a) G. De Munno, M. Julve, F. Lloret, J. Faus, A. Caneschi, J. Chem. Soc, Dalton Trans. (1994) 1175; (b) A. Rodríguez, H. Sakiyama, N. Masciocchi, S. Galli, N. Gálvez, F. Lloret, E. Colacio, Inorg. Chem. 44 (2005) 8399; (c) V. Mishra, F. Lloret, R. Mukherjee, Inorg. Chim. Acta 359 (2006) 4053; (d) O. Fabelo, J. Pasán, F. Lloret, M. Julve, C. Ruiz-Pérez, CrystEngComm 9 (2007) 815; (e) L. Cañadillas-Delgado, O. Fabelo, J. Pasán, F. S. Delgado, F. Lloret, M. Julve, C. Ruiz-Pérez, Inorg. Chem. 46 (2007) 7458; (f) O. Fabelo, J. Pasán, L. Cañadillas-Delgado, F. S. Delgado, A. Labrador, F. Lloret, M. Julve, C. Ruiz-Pérez, Cryst Growth Des. 8 (2008) 3984; (g) H. Arora, F. Lloret, R. Mukherjee, Inorg. Chem. 48 (2009) 1158; (h) O. Fabelo, J. Pasán, L. Cañadillas-Delgado, F. S. Delgado, F. Lloret, M. Julve, C. Ruiz-Pérez, Inorg. Chem. 48 (2009) 6086; (i) O. Fabelo, L. Cañadillas-Delgado, J. Pasán, F. S. Delgado, F. Lloret, J. Cano, M. Julve, C. Ruiz-Pérez, Inorg. Chem. 48 (2009) 11342; (j) O. Fabelo, J. Pasán, L. Cañadillas-Delgado, F. S. Delgado, C. Yuste, F. Lloret, M. Julve, C. Ruiz-Pérez, CrystEngComm 11 (2009) 2169.

[12] J. Cano, *VPMAG*. Revision 03, University of Valencia, Spain, 2004.

CAPTION TO THE FIGURES

Figure 1. View of the cationic heptanuclear motif in **1** along with the atom numbering scheme [Symmetry code: (′) = 1.5-*z*, 1-*x*, 0.5+*y*].

Figure 2. Detail of the packing diagram in **1** showing the H-bond interactions [Symmetry code: (″) = 0.75+*y*, 1.25-*x*, 0.75-*z*].

Figure 3. Perspective view of one of the crystallographically independent heptanuclear units in **2** along with the atom numbering scheme [Symmetry code: (′) = 1-*x*, 2-*y*, -*z*].

Figure 4. The diffuse reflectance spectra for compounds **1**, **2** and $[Co^{II}_4Co^{III}_3]$.

Figure 5. $\chi_M T$ against T plot for **1**: (o) experimental; (—) best-fit curve through the Hamiltonian of Eq (1) (see text). The inset shows the magnetization *vs. H* plot for **2** at 2.0 K. The solid line is an eye-guide.

Figure 6. $\chi_M T$ against T plot for **2**: (o) experimental; (—) best-fit curve through the Hamiltonian of Eq (2) (see text). The inset shows the magnetization *vs .H* plot for **2** at 2.0 K. The solid line is an eye-guide.

Table 1. Crystallographic data, details of data collection and structure refinement parameters for **1** and **2**.

Compound	**1**	**2**
Chemical formula	$C_{32.50}H_{63}C_{l0.75}Co_4Cu_3N_6O_{23.50}$	$C_{46}H_{74}Co_4N_2O_{24}Zn_3$
M (g mol^{-1})	1366.81	1470.90
Temperature (K)	293(2)	293(2)
Wavelength (Å)	0.71073	0.71073
Crystal system	cubic	triclinic
Space group	*I43d*	*P-1*
a (Å)	28.3682(4)	15.0941(11)
b (Å)	28.3682(4)	15.6078(12)
c (Å)	28.3682(4)	16.8004(12)
α (°)	90	71.990(6)
β (°)	90	65.560(5)
γ (°)	90	89.231(6)
V ($Å^3$)	22829.4(10)	3396.6(5)
Z	16	2
D_c (g cm^{-3})	1.591	1.438
μ (mm^{-1})	2.340	2.062
F(0 0 0)	11132	1508
Goodness-of-fit (GOF) on F^2	1.142	1.022
Final R_1, wR_2 [$I > 2\ \sigma(I)$]	0.0307, 0.0824	0.0615, 0.1575
R_1, wR_2 (all data)	0.0328, 0.0833	0.1006, 0.1743
Largest difference in peak and hole (e $Å^{-3}$)	0.491, -0,365	1.081, -0,883

Table 2. Selected bond lengths (Å) and angles (°) for **1**

Bond lengths		Bond angles	
Co1 O3	1.872(3)	O3 Co1 O2	179.29(17)
Co1 O2	1.896(3)	O3 Co1 O4	96.45(16)
Co1 O4	1.898(3)	O2 Co1 O4	83.83(15)
Co1 O1	1.935(3)	O3 Co1 O1	81.34(14)
Co1 N2	1.954(4)	O2 Co1 O1	98.02(15)
Co1 N1	1.960(4)	O4 Co1 O1	86.99(13)
Co1 Cu1	3.0271(8)	O3 Co1 N2	84.50(17)
Co2 O4	2.068(3)	O2 Co1 N2	96.17(18)
Co2 O1	2.122(3)	O4 Co1 N2	87.40(17)
Cu1 O3	1.926(3)	O1 Co1 N2	164.08(17)
Cu1 O2	1.931(3)	O3 Co1 N1	94.37(18)
Cu1 O5	1.972(4)	O2 Co1 N1	85.27(17)
Cu1 O1	2.109(3)	O4 Co1 N1	167.01(17)
Cu1 O4	2.370(4)	O1 Co1 N1	87.56(16)
		N2 Co1 N1	100.80(19)
		O3 Co1 Cu1	37.78(10)
		O2 Co1 Cu1	141.62(12)
		O4 Co1 Cu1	89.55(10)
		O1 Co1 Cu1	43.76(9)
		N2 Co1 Cu1	121.32(13)
		N1 Co1 Cu1	94.65(12)
		O4 Co2 O4	97.64(12)
		O4 Co2 O1	90.04(13)
		O4 Co2 O1	171.68(13)
		O4 Co2 O1	78.06(13)
		O4 Co2 O1	90.04(13)
		O1 Co2 O1	94.71(12)
		O3 Cu1 O5	91.11(15)
		O2 Cu1 O5	99.31(16)
		O3 Cu1 O1	75.75(13)
		O2 Cu1 O1	94.18(14)
		O5 Cu1 O1	165.55(14)
		O3 Cu1 O4	102.83(14)
		O2 Cu1 O4	71.39(13)
		O5 Cu1 O4	106.51(13)
		O1 Cu1 O4	82.65(11)
		O3 Cu1 Co1	36.53(10)
		O2 Cu1 Co1	133.02(12)
		O5 Cu1 Co1	127.63(11)
		O1 Cu1 Co1	39.40(8)
		O4 Cu1 Co1	91.11(8)

Table 3. Selected bond lengths (Å) and angles (°) for **2** (first unit)

Bond lengths		Bond angles	
Co3 O14	1.874(4)	O14 Co3 O15	90.04(19)
Co3 O15	1.887(4)	O14 Co3 N2	86.8(2)
Co3 N2	1.904(5)	O15 Co3 N2	89.0(2)
Co3 O16	1.906(4)	O14 Co3 O16	173.1(2)
Co3 O1B	1.919(5)	O15 Co3 O16	86.79(19)
Co3 O1M	1.920(4)	N2 Co3 O16	87.0(2)
Co3 Co4	2.9509(11)	O14 Co3 O1B	91.9(2)
Co3 Zn1	2.9948(9)	O15 Co3 O1B	177.4(2)
Co4 O12	2.017(5)	N2 Co3 O1B	92.7(2)
Co4 O14	2.050(4)	O16 Co3 O1B	91.41(19)
Co4 O13	2.057(5)	O14 Co3 O1M	88.66(18)
Co4 O11	2.133(4)	O15 Co3 O1M	86.09(18)
Co4 O1M	2.165(4)	N2 Co3 O1M	173.3(2)
Co4 O33	2.0915(68)	O16 Co3 O1M	97.29(18)
Zn1 O1M	2.041(4)	O1B Co3 O1M	92.32(19)
Zn1 O15	2.101(4)	O12 Co4 O13	94.5(2)
Zn1 O11	2.129(4)	O14 Co4 O13	87.28(19)
Zn1 Co3	2.9948(9)	O12 Co4 O11	94.24(19)
Zn2 O11	1.954(4)	O14 Co4 O11	82.72(17)
Zn2 O15	2.453(4)	O13 Co4 O11	166.67(17)
Zn2 O17	1.971(5)	O12 Co4 O1M	94.5(2)
Zn2 O18	1.986(5)	O14 Co4 O1M	77.90(16)
Zn2 O16	1.998(5)	O13 Co4 O1M	87.18(18)
		O11 Co4 O1M	82.14(15)
		O11 Zn1 O11	180.0
		O11 Zn2 O17	113.1(2)
		O11 Zn2 O18	113.5(2)
		O17 Zn2 O18	96.6(2)
		O11 Zn2 O16	115.11(18)
		O17 Zn2 O16	119.1(2)
		O18 Zn2 O16	96.5(2)

O11 Zn2 O15	76.94(15)
O17 Zn2 O15	86.36(18)
O18 Zn2 O15	166.6(2)
O16 Zn2 O15	70.83(16)

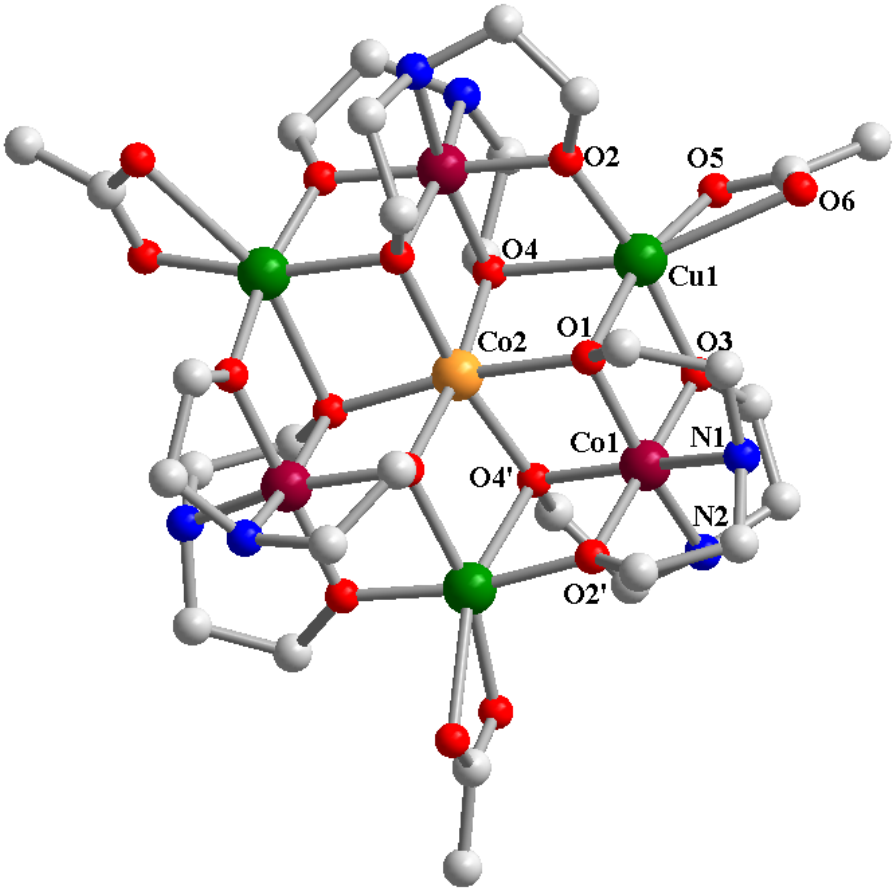

Figure 1

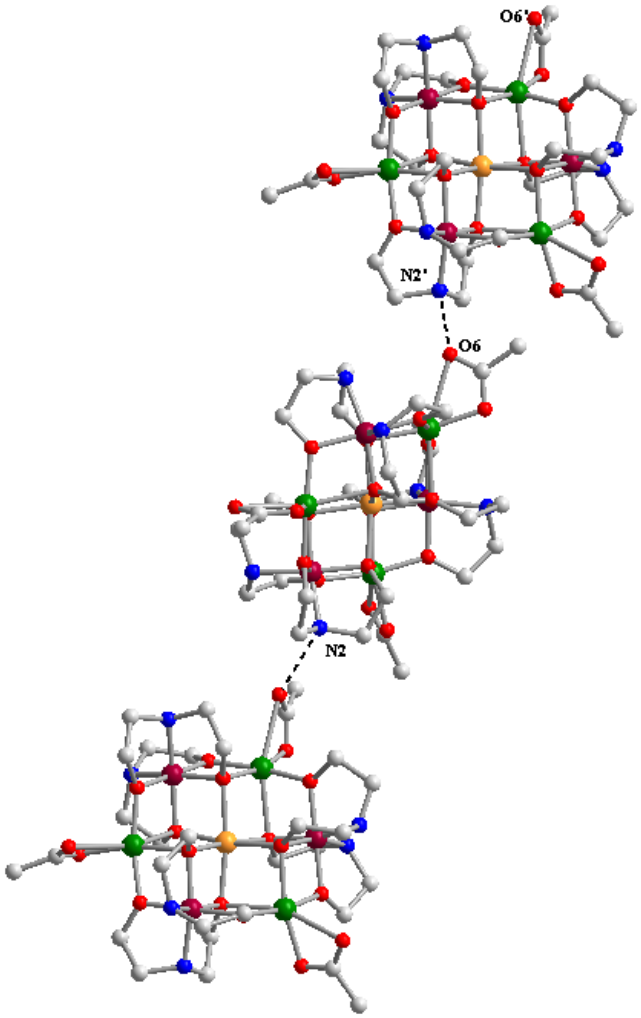

Figure 2

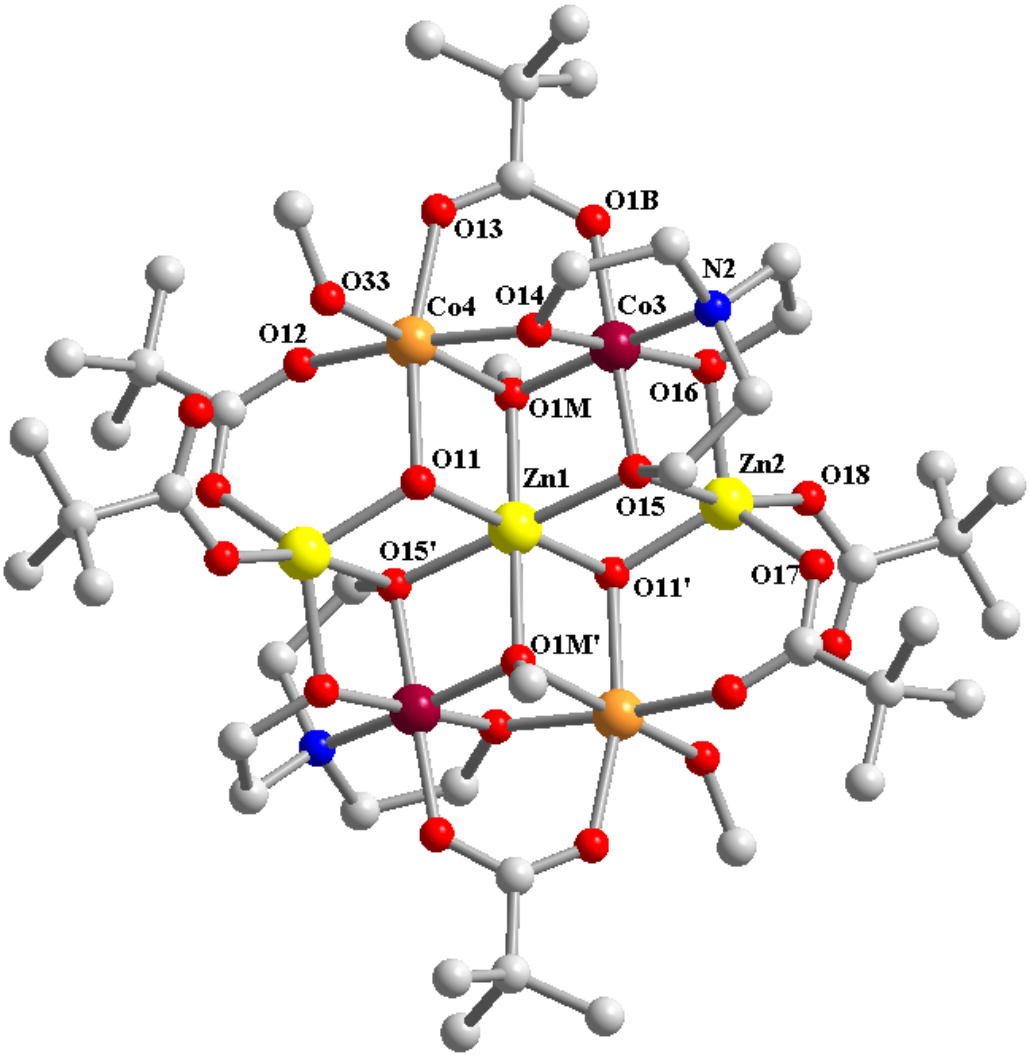
O1B
O13
O33
Co4
O14
Co3
N2
O12
O1M
O16
O11
Zn1
Zn2
O18
O15
O15'
O11'
O17
O1M'

Figure 3

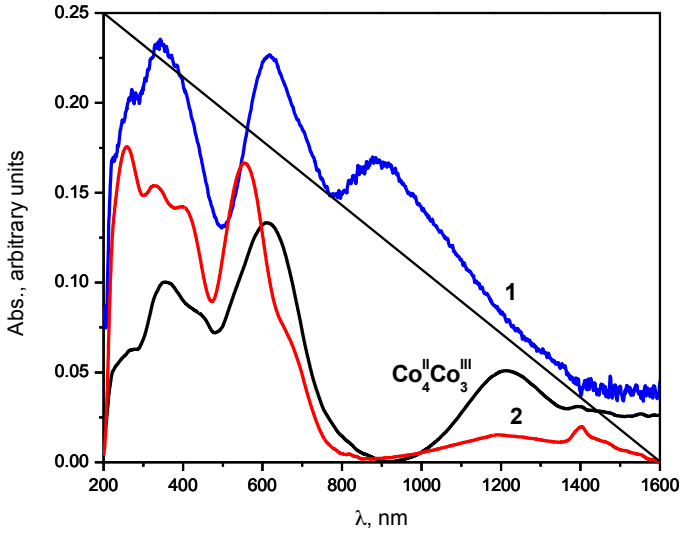

Figure 4

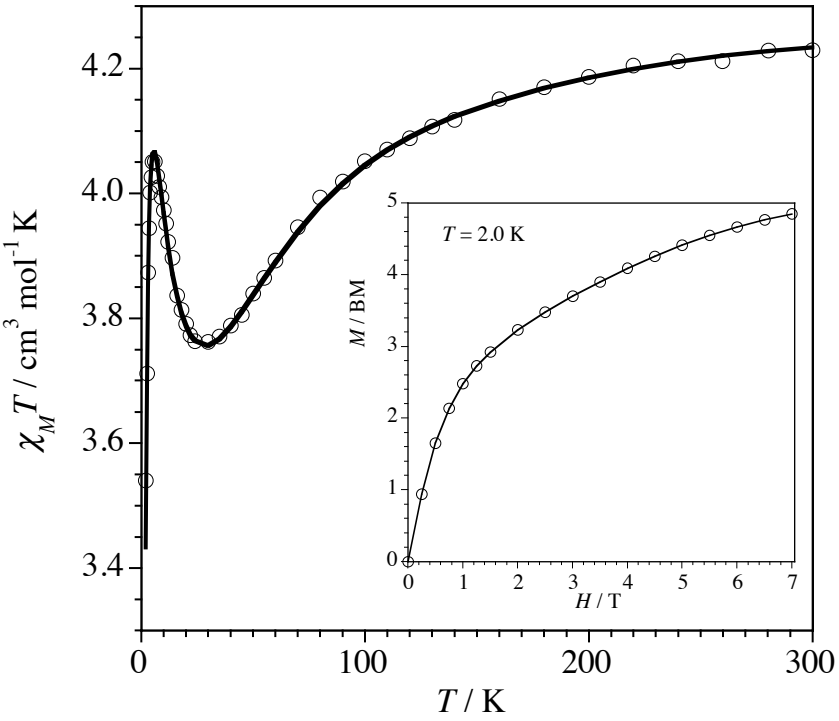

Figure 5

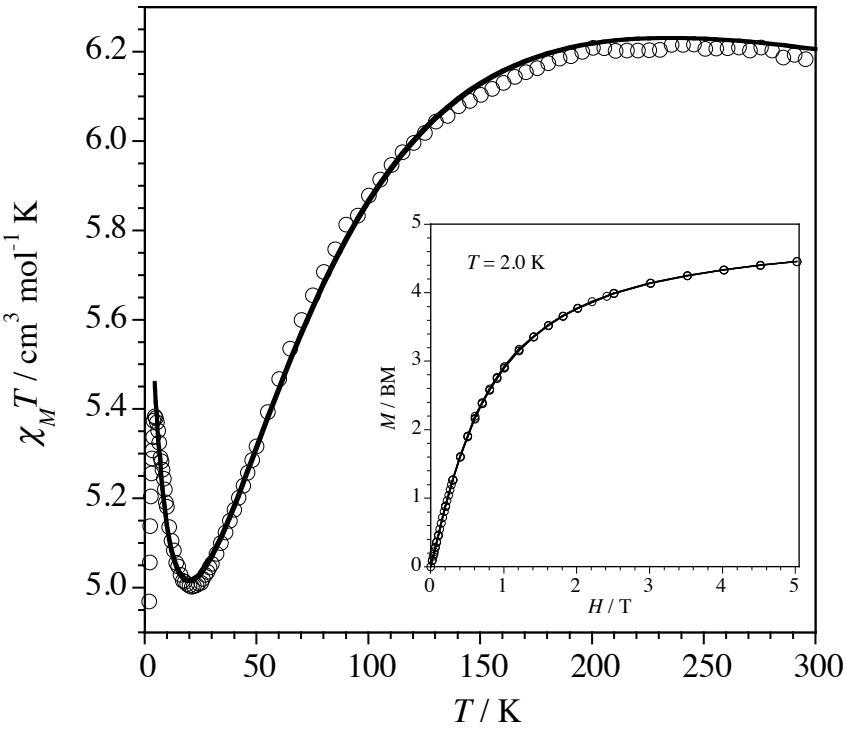
6.2
6.0
5.8
5.6
5.4
5.2
5.0
$\chi_M T$ / cm^3 mol^{-1} K
0
50
100
150
200
250
300
T / K
T = 2.0 K
M / BM
H / T
0
1
2
3
4
5

Figure 6